# Candidates for direct laser cooling of diatomic molecules with the simplest $^{1}\Sigma$-$^{1}\Sigma$ electronic system

Chuanliang Li, Yachao Li, Zhonghua Ji, Xuanbing Qiu, Yunzhong Lai, Jilin Wei, Yanting Zhao, Lunhua Deng, Yangqin Chen, and Jinjun Liu

# Candidates with the simplest $^1\Sigma$ - $^1\Sigma$ electronic system for direct laser cooling of diatomic molecules

Chuanliang Li[1],[*] Yachao Li[1], Zhonghua Ji[2,3], Xuanbing Qiu[1],
Yunzhong Lai[1], Jilin Wei[1], Yanting Zhao[2,3],[†] Lunhua Deng[4], Yangqin Chen[4], and Jinjun Liu[5][‡]

[1]*Department of Physics, School of Applied Science,*
*Taiyuan University of Science and Technology, Taiyuan 030024, China*
[2]*State Key Laboratory of Quantum Optics and Quantum Optics Devices,*
*Institute of Laser Spectroscopy, Shanxi University, Taiyuan 030006, China*
[3]*Collaborative Innovation Center of Extreme Optics,*
*Shanxi University, Taiyuan, Shanxi 030006, China*
[4]*State Key Laboratory of Precision Spectroscopy,*
*East China Normal University, Shanghai 200062, China and*
[5]*Department of Chemistry, University of Louisville, Louisville, Kentucky 40292, USA*

We propose to utilize the $^1\Sigma$ - $^1\Sigma$ electronic transition system for direct laser cooling of heteronuclear diatomic molecules. AgH, as well as its deuterium isotopologue AgD, is used as an example to illustrate the cooling schemes. Potential energy curves and relevant molecular parameters of both AgH and AgD, including the spin-orbit constants and the electronic transition dipole moments, are determined in internally contracted multiconfiguration-reference configuration interaction calculations. The highly diagonal Franck-Condon matrices of the $A^1\Sigma^+$ - $X^1\Sigma^+$ transitions predicted by the calculations suggest the existence of quasi-closed-cycle transitions, which renders these molecules suitable for direct laser cooling. By solving rate equations numerically, we demonstrated that both AgH and AgD molecules can be cooled from 25 K to 2 mK temperature in approximately 20 milliseconds. Our investigation elucidates and supports the hypothesis that molecules in the simplest $^1\Sigma$ - $^1\Sigma$ system can serve as favorable candidates for direct laser cooling.

PACS numbers: 32.70.Ca, 37.10.Mn, 31.15.A-

## I. INTRODUCTION

In the past three decades, laser cooling of atoms has allowed access to ultracold temperature and opened up new frontiers of physics [1–3]. Built on the progress on (ultra)cold atoms, ultracold molecules, especially the polar ones, have gained increasing attention. Compared to ultracold atoms, ultracold polar molecules possess many special properties. For example, they are often subject to tunable, long-range and anisotropic dipole-dipole interactions and therefore constitute an ideal testbed for the study of many-body physics [4]. Ultracold polar molecules also have broad potential applications in ultracold chemistry [5, 6], precision measurements [7, 8], and quantum computation [9].

To date, the most effective approach to producing ultracold molecules is to start from precooled atoms and form ultracold molecules by magnetoassociation [10] or photoassociation [11]. However, ultracold molecules formed in this way are limited to bialkali and alkali-alkaline earth molecules. The production efficiency is low and the ultracold molecules are formed in weakly bound states. Although a two-photon stimulated Raman adiabatic passage (STIRAP) process can alleviate these problems, it increases the complexity of experimental apparatuses. A more versatile and potentially more feasible alternative to producing ultracold molecules is direct free-space laser cooling and trapping, similar to Doppler cooling atoms. Laser cooling of molecules is significantly more complicated than atoms due to complex rovibrational structure of molecules, preventing the use of conventional schemes for cooling atoms [12]. Therefore, it is critical to seek candidate molecules with quasi-closed-cycle transitions that are analogous to those for cooling atoms. To achieve a high cooling efficiency, spontaneous decays from states involed in the closed-cycle transitions to other states out of the cycle should be avoided. Guided by the laser cooling criteria [13], schemes for cooling many diatomic neutrals, such as RaF [14], AlH [15], AlF [15], BeF [16], MgF [17], GaF [18] and BH [18], have been proposed. Experimentally, significant progress has been made over the past years in direct laser cooling and magneto-optical trapping of diatomic molecules including SrF [19], YO [20, 21] and CaF [22, 23]. Most recently, direct laser-cooling of diatomic cations have also been proposed [24]. Laser cooling of molecular ions has its unique advantages because of their long storage time and spatial localization in the ion trap, which allow multi-step cooling.

Most theoretical proposals and all experimental implementations thus far utilize the $^2\Pi$ - $^2\Sigma^+$ electronic transition system for laser cooling. Because of the spin multiplicity, rotational energy levels in both the $^2\Sigma^+$ and $^2\Pi$ states are split by the spin-rotation interaction. The $^2\Pi$ state, being orbitally doubly degenerate, is further

---

FIG. 1. (Color online) Laser-cooling schemes for AgH and AgD molecules in the $A^1\Sigma^+$ - $X^1\Sigma^+$ system. The dash lines and solid lines represent spontaneous emission and excited lasers, respectively. (a) Using the $(J' = 1 \leftarrow J'' = 0)$ transition, (b) using the $(J' = 0 \leftarrow J'' = 1)$ transition.

the present work, two molecules, AgH and its deuterium isotopologue (AgD), are used as examples to demonstrate the cooling scheme utilizing a $^1\Sigma^+$ - $^1\Sigma^+$ transition. AgH and AgD have a simple $^1\Sigma^+$ ground electronic state because of their closed subshells. Rotationally resolved $A^1\Sigma^+$ - $X^1\Sigma^+$ transitions of both AgH [25] and AgD [26] were recorded in the near-UV region and analyzed in the early ages of quantum mechanics. More extensive investigation of the vibronic transitions in the $A^1\Sigma^+$ - $X^1\Sigma^+$ system of AgH was performed by Gerö and Schmid [27]. Later, Learner explained the irregularities in the vibrational intervals and the intensity distribution in terms of perturbation between different $^1\Sigma^+$ states and the vibration-rotation interaction [28]. Ground-state vibrational structure of AgH and AgD was studied in both tunable diode laser absorption spectroscopy [29] and Fourier-transform emission spectroscopy [30]. Witek et al. first calculated potential energy curves (PECs) of ground and low-lying excited electronic states of AgH using the relativistic all-electron multireference-based perturbation technique [31, 32]. In a global direct-potential-fit analysis of UV, IR and microwave spectra of multiple isotopologues, Le Roy et al. determined the analytic potential-energy functions and the Born-Oppenheimer breakdown radial functions for the $X^1\Sigma^+$ and $A^1\Sigma^+$ states [33]. These spectroscopic and theoretical investigations provide accurate and comprehensive descriptions of PECs, energy level structure, and transition intensities of AgH and AgD, indispensable information to developing practical laser cooling schemes.

In addition to utilizing results from previous experimental and computational investigations, we carried out internally contracted multiconfiguration-reference configuration interaction (MRCI) calculations to predict molecular constants and properties of AgH and AgD relevant to laser cooling. Calculated molecular parameters are used in solving the rate equations and to simulate the laser-cooling process. On the basis of calculations and simulation with AgH and AgD, the prospect of direct laser cooling of diatomic molecules using the $^1\Sigma^+$ - $^1\Sigma^+$ electronic transition system in general will be discussed.

## II. COOLING SCHEMES

Before quantitative simulation and detailed discussion, which will be presented in the following sections, the proposed schemes for laser-cooling AgH and AgD molecules will be outlined. Generally speaking, the criteria of selecting candidate molecules and transitions for laser cooling include [13, 34] (1) an electronic transition with large oscillator strength to ensure a sufficient photon scattering rate for rapid laser cooling, (2) the availability of lasers in the frequency range of the selected electronic transition [35], (3) a highly diagonal Franck-Condon (FC) factor matrix for transitions between vibrational levels of the involved electronic states, and (4) absence of intermediate state that may terminate the cooling cycle through

subject to the spin-orbit interaction and the $\Lambda$-type doubling, which arises from coupling of molecular rotation and the electronic orbital angular momentum. Due to the additional, often nearly degenerate energy levels that can be populated during the cooling process, re-pumping lasers are required to return the population to the cooling cycle. Therefore, simple electronic transition systems in diatomic molecules that satisfy laser cooling criteria are strongly desired.

The $^1\Sigma$ state has the simplest rotational structure of all electronic states of molecules due to the absence of spin multiplicity and orbital degeneracy. Many angular momentum coupling mechanisms that are ubiquitous in open-shell molecules vanish in $^1\Sigma$ state molecules. In

population leakage. The last two criteria are imposed to limit the number of lasers necessary for laser cooling. Following these criteria, we verify the practicability of laser-cooling the AgH molecule utilizing its $A^1\Sigma^+$ - $X^1\Sigma^+$ system.

(1) The $A^1\Sigma^+$ - $X^1\Sigma^+$ transition of AgH corresponds to an electron promotion from the $5s$ orbital of the silver atom to its $5p$ orbital, both of which are only slightly perturbed by the Ag-H bond. Because of its atomic-like nature, this transition has a large transition dipole moment (TDM) of 2.63 Debye.

(2) External-cavity diode lasers (ECDLs) are the most commonly used in direct laser cooling. The electronic term value ($T_e$) of the $A^1\Sigma^+$ - $X^1\Sigma^+$ transition of AgH is 29959.0 cm$^{-1}$ ($\lambda \sim 330$ nm) [36]. Thus far, the shortest wavelength that can be covered by direct output from commercially available ECDLs is around 370 nm. However, frequency-doubled ECDLs or ring-cavity dye lasers can be used to excite the cooling and re-pumping transitions. Moreover, short-wavelength diode lasers have been actively pursued and ECDLs around 330 nm may be available in the near future.

(3) The atomic-like nature of the $X^1\Sigma^+$ - $A^1\Sigma^+$ transition of AgH also leads to close internuclear distances ($R_e$) and harmonic frequencies ($\omega_e$) for the $X^1\Sigma^+$ and $A^1\Sigma^+$ states. Therefore, the FC matrix is highly diagonal for transitions between low vibrational energy levels of these two electronic states. Since molecules populate the ground vibrational ($v'' = 0$) level of the $X^1\Sigma^+$ state almost exclusively under laser-cooling experimental conditions, the $v' = 0 \leftarrow v'' = 0$ transition can be used for laser cooling. The relative intensity of the $A^1\Sigma^+ \rightarrow X^1\Sigma^+$ vibronic transitions and, hence, the relative decay rates of the excited-state population from the $A^1\Sigma^+(v' = 0)$ level to different vibrational levels of the $X^1\Sigma^+$ state through spontaneous emission, are determined by FC factors. Both experimental [37] and computational (Section III B) results suggest that radiative relaxation from the $v' = 0$ level is dominated by transitions to the $v'' = 0$ and $v'' = 1$ levels. Transitions to other ground-state vibrational levels are negligible. Re-pumping lasers are therefore necessary to excite transitions in the $A^1\Sigma^+$ - $X^1\Sigma^+(0,0)$ and $(0,1)$ vibronic bands to return the population to the cooling cycle.

(4) There is no *singlet* electronic state between the $A^1\Sigma^+$ and $X^1\Sigma^+$ states of AgH to which radiative transitions from the $A^1\Sigma^+$ state are possible. Additionally, $v'' \geq 1$ levels of the ground electronic state have a long lifetime (see Section III B) so that vibrational relaxation from $v'' \geq 1$ levels is insignificant. Rotational relaxation in the ground electronic state is negligible. Taken together, these three factors ensure that population leakage can be prevented with only one or three re-pumping lasers for laser cooling using the $A^1\Sigma^+$ - $X^1\Sigma^+$ system.

Prior to direct laser cooling, internal-state cooling is necessary to prepare molecules on limited number of rotational energy levels. Given the rotational constants of AgH (6.449 cm$^{-1}$) [36] and AgD (3.2229 cm$^{-1}$) [26],

both the $J'' = 0$ and the $J'' = 1$ rotational levels of the $X^1\Sigma^+$ state have considerable population under typical pre-laser-cooling conditions (cryogenic buffer-gas cooling [19–21] or supersonic jet expansion [22]). Assuming a rotational temperature of 3 K, population on the $J'' = 1$ level is 0.21% and 4.5% of that on the lowest rotational ($J'' = 0$) level for AgH and AgD, respectively. It is therefore advantageous to laser-cool molecules on the $J'' = 0$ level when the density of molecules is considered. However, the number of lasers required to cool molecules on the $J'' = 1$ level is significantly smaller than the $J'' = 0$ level. This is because, limited by the rotational selection rule for a $\Sigma^+$ - $\Sigma^+$ electric dipole transition, namely $\Delta J = \pm 1$, the only allowed transition for molecules on the $J'' = 0$ level is to the $J' = 1$ level, i.e., the R(0) transition. Thereafter, molecules on the $v' = 0, J' = 1$ level can decay *via* spontaneous emission to not only the $J'' = 0$ but also the $J'' = 2$ rotational levels of the $v'' = 0$ vibrational state, corresponding to the R(0) and P(2) transitions, respectively. In addition, transitions from the $v' = 0, J' = 1$ level to the $J'' = 0$ and $J'' = 2$ levels of the $v'' = 1$ state are allowed. Three re-pumping lasers are therefore necessary to return the population on the $J'' = 2$ level of the $v'' = 0$ state and the $J'' = 0, 2$ levels of the $v'' = 1$ state to the cooling cycle as plotted in Fig. 1a. The cooling and re-pumping transitions form a "$\Lambda$" system.

By comparison, if one chooses to laser-cool molecules on the $(v'' = 0, J'' = 1)$ level by exciting the $J' = 0 \leftarrow J'' = 1$, i.e., the P(1) transition in the (0,0) band, the only allowed subsequent $A^1\Sigma^+ \rightarrow X^1\Sigma^+$ transitions *via* spontaneous emission are those to the $J'' = 1$ levels. Again, limited by FC factors, spontaneous emission from the $v' = 0$ level to all vibrational levels of the $X^1\Sigma^+$ state except $v'' = 0$ and 1 may be neglected. As a result, only one re-pumping laser for the excitation of the $(v' = 0, J' = 0) \leftarrow (v'' = 1, J'' = 1)$ transition is required in this laser-cooling scheme (Fig. 1b). We will discuss details of these two cooling schemes using experimental and calculated results in the following sections.

Finally, we consider the hyperfine structure of the candidate molecules. AgH as well as AgD is a closed-shell molecule in which the *magnetic* hyperfine interaction vanishes. Because of difference in the nuclear spin quantum numbers of H ($I = 1/2$) and D ($I = 1$), only AgD has a nonzero nuclear quadrupole-coupling parameter ($eQ_q$). As a result, only AgD has nondegenerate hyperfine sublevels. Nonetheless, $eQ_q$ for AgD is small, predicted to be $\sim 0.07$ MHz in a coupled cluster calculation [38]. Therefore, the hyperfine structure of each rotational transition can be covered by a single-laser output.

In comparison, the total nuclear spin of normal isotopologues of all three molecules that have been laser-cooled thus far, namely, $^{88}_{38}$Sr$^{19}_9$F, $^{89}_{39}$Y$^{16}_8$O and $^{40}_{20}$Ca$^{19}_9$F, is $I = 1/2$. Since the total electron spin $S$ is also $1/2$ for these molecules, there are four hyperfine sublevels for each rotational level except $N = 0$, which splits to three hyperfine sublevels. In direct laser cooling, side-

bands generated from ECDL-pumped electro-optic modulators (EOMs) and acousto-optic modulators (AOMs) are used to address allowed transitions between hyperfine sublevels.

To summarize, the number of wavelengths needed to laser-cool AgH as well as AgD molecules on the $J'' = 0$ and $J'' = 1$ levels of the $X^2\Sigma^+(v'' = 0)$ state is four and two, respectively. Each wavelength can be generated by frequency doubling of an ECDL or ring-cavity dye laser. There is no need to generate sidebands using AOMs or EOMs to address transitions between hyperfine sublevels. The total number of wavelengths required to laser-cool AgH and AgD is therefore significantly less than those used in laser-cooling molecules in the $^2\Pi$ - $^2\Sigma^+$ transition system.

## III. CALCULATIONS

*Ab initio* calculations were carried out using Molpro2012 software package [39]. Although silver has two stable isotopes with close nature abundances, namely, $^{107}$Ag and $^{109}$Ag, only $^{107}$Ag is considered in the calculations. The difference between energy level structures of $^{107}$AgH ($^{107}$AgD) and $^{109}$AgH ($^{109}$AgD) is insignificant because the reduced mass of AgH (AgD) is determined almost entirely by the mass of H (D) and both $^{107}$Ag and $^{109}$Ag have a nuclear spin of $I = 1/2$.

AgH is a heteronuclear diatomic molecule and belongs to the $C_{\infty v}$ point group. It has six low-lying electronic states dissociating to the Ag($^2S_g$)+H($^2S_g$) and Ag($^2P_u$)+H($^2S_g$) atomic limits: $X^1\Sigma^+$, $a'^3\Sigma^+$, $A^1\Sigma^+$, $a^3\Pi$, $b'^3\Sigma^+$, and $C^1\Pi$. They are labeled as $X^1\Sigma^+$, $1^3\Sigma^+$, $2^1\Sigma^+$, $1^3\Pi$, $2^3\Sigma^+$, and $1^1\Pi$ states in Ref. [31], respectively. The active space used in the calculation consists of eight molecular orbitals corresponding to the $4d$, $5s$ and $5p\sigma$ orbitals of Ag and the $1s$ orbital of H. The symmetries of the molecular orbitals included in the active space are as follows: five with $a_1$ symmetry, one $b_1$, one $b_2$, and one $a_2$. The $4s$ and $4p$ orbitals of Ag are closed but non-frozen in the calculations. Wavefunctions of the valence electrons are optimized by the state-averaged complete active space self-consistent field (SA-CASSCF) method following a Hartree-Fock calculation. Subsequently, the SA-CASSCF wavefunctions are used in the internally contracted MRCI calculation [40]. At its equilibrium, the ground ($X^1\Sigma^+$) state arises mainly from the configuration of $\dots 10\sigma^2 11\sigma^2 5\pi_x^2 5\pi_y^2 2\delta^2 12\sigma^1 13\sigma^1 14\sigma^0$ (96.4%). The first ($A^1\Sigma^+$) and the lowest triplet electronic state ($a'^3\Sigma^+$) are generated by the promotion of an electron from the $5\pi_x$ and $12\sigma$ orbitals, respectively, to the $14\sigma$ orbital.

To improve the accuracy of PEC calculations, the effects of the core-valence correction and the relativistic correlation are taken into account. This was done by adopting the ecp28mdf basis set for Hg and the aug-cc-pVTZ basis set for H, and the Douglas-Kroll Hamiltonian approximation [41–43]. The PEC scan ranges from 0.8
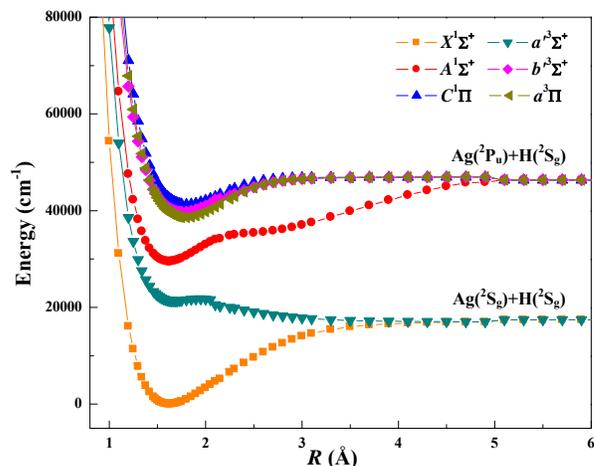


FIG. 2. (Color online) Potential energy curves of low-lying electronic states of AgH and AgD.

to 8.0 Å in internuclear distance. A stepsize of 0.05 Å was used except around the equilibrium of the ground state, where it was reduced to 0.01 Å. The equilibrium internuclear distances $R_e$ are determined in fitting the PEC near the equilibrium (see Table I). Also calculated were permanent dipole moment $[\mu(r)]$ of each electronic state and electric TDMs between the ground and excited electronic states. Both quantities are dependent on the internuclear distance ($r$).

Using the *ab initio* calculated PECs, rovibrational energy levels of aforementioned electronic states were calculated using the LEVEL program, which solves the radial one-dimension Schrödinger equations of nuclear motion using the Numerov method [44]. $\omega_e$ and the anharmonicity coefficient ($\omega_e\chi_e$) are determined in fitting the vibrational energy levels. The LEVEL program also calculates the rotational constants of vibrational energy levels ($B_v$), from which the rotational constant at the equilibrium $B_e$ can be determined. The same program provides FC matrices, and TDMs between rovibrational energy levels of different electronic states, and, hence, the Einstein A coefficients. Computational results are presented in Table I and discussed in the rest of the present section.

### A. Potential energy curves and spectroscopic constants

PECs of the six lowest-energy electronic states of AgH calculated in the present work ($X^1\Sigma^+$, $A^1\Sigma^+$, $C^1\Pi$, $a'^3\Sigma^+$, $a^3\Pi$ and $b'^3\Sigma^+$) are shown in Fig. 2. The ground triplet ($a'^3\Sigma^+$) state, the only intermediate electronic state between the $X^1\Sigma^+$ and $A^1\Sigma^+$ states, is weakly bound. Its PEC features a shallow well and does not hold any vibrational levels according to the calculation. It is split by the spin-orbit interaction into one $\Omega = 0^-$ component and two degenerate $\Omega = 1$ components. Energy separation between the PECs of these spin-orbit states $\Delta E_{\Omega=1-\Omega=0^-}$ is calculated to be 4.56 cm$^{-1}$ at the equi-

TABLE I. Spectroscopic constants for the $X^1\Sigma^+$, $A^1\Sigma^+$, $C^1\Pi$, $a^3\Pi$ and $b'^3\Sigma^+$ states of AgH and AgD. $T_e$: electronic transition frequency. $D_e$: dissociation energy. Other symbols are defined in the text.

| Molecules | States | $T_e(cm^{-1})$ | $R_e(\text{Å})$ | $B_e(cm^{-1})$ | $D_e(\text{eV})$ | $\omega_e(cm^{-1})$ | $\omega_e\chi_e(cm^{-1})$ | Ref. |
|---|---|---|---|---|---|---|---|---|
| AgH | $X^1\Sigma^+$ | 0 | 1.6177 | 6.44647 | 2.16 | 1634.2 | 35.23 | This work |
| | | 0 | 1.564 | 6.904 | 2.52 | 2073 | 52.7 | Cal.[32] |
| | | | 1.62 | 6.43 | | 1902 | | Cal.[31] |
| | | | 1.6174 | 6.499 | 2.38 | 1759.9 | 34.18 | Cal.[33] |
| | | 0 | 1.6172 | 6.45 | | 1759.7 | 33.97 | Exp.[45] |
| | $A^1\Sigma^+$ | 29500 | 1.6412 | 6.263 | 2.34 | 1659.7 | 122 | This work |
| | | 32208 | 1.717 | 5.73 | 2.30 | 1422 | 27.3 | Cal.[32] |
| | | | 1.604 | 6.56 | | 1805 | | Cal.[31] |
| | | 29959 | 1.638,1.665 | 6.265 | 2.36 | 1663.6 | 87 | Exp.[28, 46] |
| | $C^1\Pi$ | 41274 | 1.7875 | 5.28 | 0.63 | 1477 | 69 | This work |
| | | 41261 | 1.6 | 6.54 | | 1589 | 42 | Exp.[28] |
| | $a^3\Pi$ | 38601 | 1.7626 | 5.43 | 0.96 | 1502 | 21.1 | This work |
| | | 44305 | 1.594 | 6.644 | 0.91 | 1620 | 89.4 | Cal.[32] |
| | | | 1.594 | 6.64 | | 1742 | | Cal.[31] |
| | | 41700 | <1.64 | >6.3 | 1.20 | 1450 | 50 | Exp.[28] |
| | $b'^3\Sigma^+$ | 39743 | 1.7466 | 5.53 | 0.82 | 1603 | 103 | This work |
| AgD | $X^1\Sigma^+$ | 0 | 1.6173 | 3.25736 | 2.16 | 1178.4 | 21.13 | This work |
| | | 0 | 1.618 | 3.2572 | | 1250.7 | 17.17 | Exp.[28] |
| | $A^1\Sigma^+$ | 29500 | 1.6325 | 3.197 | 2.34 | 1072.75 | 47.04 | This work |
| | | 29960 | 1.644 | 3.154 | | 1160.82 | 31.73 | Exp.[28] |
| | $C^1\Pi$ | 41274 | 1.7847 | 2.675 | 0.63 | 1056 | 36 | This work |
| | | 41269 | 1.599 | 3.335 | | 1108 | 25 | Exp.[28] |
| | $a^3\Pi$ | 38601 | 1.7732 | 2.71 | 0.96 | 1067 | 11 | This work |
| | | 41700 | <1.6 | >3.2 | | 1040 | 25 | Exp.[28] |
| | $b'^3\Sigma^+$ | 39743 | 1.74 | 2.8 | | | | This work |

librium. PECs of the other two triplet states calculated, namely, the $a^3\Pi$ and $b'^3\Sigma^+$ state, almost overlap with the $C$ state.

Calculated spectroscopic constants for AgH as well as AgD in each electronic state are listed in Table I in comparison with previous experimental and computational results. $R_e$'s of the $X^1\Sigma^+$ and $A^1\Sigma^+$ states are very close: 1.616 and 1.641 Å, respectively. In addition, harmonic frequencies ($\omega_e$) of $X^1\Sigma^+$ and $A^1\Sigma^+$ are similar to each other for both AgH and AgD. They suggest a highly diagonal FC matrix for vibronic transitions between these two states. In general, spectroscopic constants calculated in the present work are consistent with previous experimental and calculated results [28, 31–33, 45, 46]. Compared to *ab initio* calculations by Witek *et al.* [31, 32], our results for the $X^1\Sigma^+$ and the $A^1\Sigma^+$ states of AgH are in better agreement with experimentally determined values. To the best of our knowledge, there was no previous *ab initio* calculation on molecular constants of the $b'^3\Sigma^+$ state of AgH. Furthermore, electronic states and molecular constants of AgD are calculated for the first time in the present work. Again, our calculated values on AgD are in good agreement with experimental values [28].

Given $T_e$ and the vibrational frequencies, the wavelengths of the cooling and re-pumping lasers for AgH are 338.4 nm and 357.9 nm. They are 338.6 nm and 352.4 nm for AgD (see Fig. 3).

It is worth noting that *ab initio* calculations predict that the $a'^3\Sigma^+$ state lying between the $A^1\Sigma^+$ and $X^1\Sigma^+$ states is dissociative, which potentially poses an additional channel for population leakage in laser cooling. However, the transition of $^3\Sigma^+$ - $^1\Sigma^+$ is spin-forbidden. It gains intensity through spin-orbit coupling between the $A^1\Sigma^+$ and the $a'^3\Sigma^+$ states, which can be evaluated by means of full one- and two-electron Breit-Pauli operator. The electronic transition dipole moment for the $A^1\Sigma^+$ - $a'^3\Sigma^+$ transition is calculated to be $1.69 \times 10^{-2}$ Debye and is two orders of magnitude weaker than that of the $A^1\Sigma^+$ - $X^1\Sigma^+$ transition.

## B. FC factors, Einstein coefficients and radiative lifetimes

FC factors ($f_{v'v''}$) for the $A^1\Sigma^+$ - $X^1\Sigma^+$ system of AgH and AgD are sketched in Fig. 4(a) and 4(b), respectively. Numerical values are tabulated in the Supplemental Materials. It is obvious that the diagonal ($\Delta v = 0$) elements have significantly larger values. The FC factor for the origin, i.e., (0, 0) vibronic band of the $A^1\Sigma^+$ - $X^1\Sigma^+$ system, denoted with $f_{00}$, is 99.5% for both AgH and AgD. The off-diagonal FC factor $f_{01}$ is approximately 0.5% for AgH and AgD, whereas all other off-diagonal FC factors for $v' = 0 \rightarrow v'' > 1$ transitions are essentially zero (see Supplementary Materials). Average total number of scattering events before a molecule decays to $v'' \geq 2$ vibrational levels of the $X^2\Sigma^+$ state is equal to inverse of the sum of the FC factors for vibronic transitions
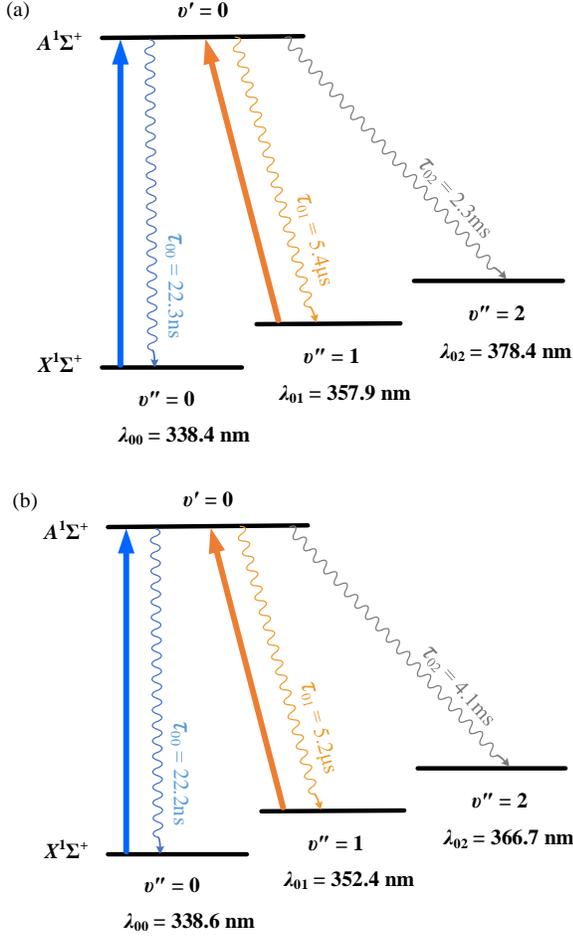
FIG. 3. (Color online) Cooling scheme for AgH (a) and AgD (b) molecules with the $A^1\Sigma^+$ - $X^1\Sigma^+$ system. The wavelengths and radiative lifetimes are labeled for each transition.

to these levels: ($\langle N_{photon} \rangle = \left( \sum\limits_{v'' \geq 2} f_{0v''} \right)^{-1}$). Using the calculated FC factors, $\langle N_{photon} \rangle$ is $\sim 5{,}000$ for AgH and $\sim 15{,}000$ for AgD. Therefore, AgH and AgD satisfy the third criterion for potential laser-cooling candidates. Of note, $f_{00}$ of AgH and AgD are larger than or close to other diatomics that have been laser-cooled in experiment or investigated theoretically as candidate molecules such as MgF (0.917) [17], SrF (0.98) [47], TiO (0.845) [34], YO (0.9944) [20] and LiRb (0.998) [48].

The first and third criteria for laser cooling of molecules (see Section II) demand strong cooling as well as re-pumping transitions, which ensures sufficient spontaneous scattering force for decelerating the molecule. The line strength of the transition between two rotational energy levels is directly related to the Einstein $A$ coefficient and, hence, the nature lifetime of the upper level. The Einstein $A$ coefficient for a ro-vibronic transition in

spontaneous emission can be calculated as [44, 49].

$$A_{i \rightarrow j} = 3.1361891 \times 10^{-7} \frac{S(J', J'')}{2J' + 1} v_{ij}^3 |\langle \Psi_i | \hat{\mu}(r) | \Psi_j \rangle|^2 \tag{1}$$

where $i$ and $j$ are to label the initial (upper) and the final (lower) energy levels, respectively. $S(J', J'')$ is the Hönl-London rotational intensity factor. $\nu_{ij}$ is the transition frequency in cm$^{-1}$. $M(r) = \langle \Psi_i | \hat{\mu}(r) | \Psi_j \rangle$ is the TDM, where $\hat{\mu}$ is the electric dipole operator in the unit of Debye, and $\Psi_i$ and $\Psi_j$ are the vibronic wavefunctions of the $i$ and $j$ levels, respectively. $\hat{\mu}$ and, hence, $M$ are dependent on the internuclear distance. The Einstein coefficient $A$ calculated using Eq. 1 is in the unit of $s^{-1}$.

Time constants for spontaneous emission, i.e., $\tau_{ij} = A_{i \rightarrow j}^{-1}$, of the $(v' \rightarrow v'') = (0 \rightarrow 0)$, $(0 \rightarrow 1)$ and $(0 \rightarrow 2)$ vibronic transitions in the $A^1\Sigma^+$ - $X^1\Sigma^+$ system of AgH are calculated to be 22.3 ns, 5.4 $\mu$s and 2.33 ms, respectively (see Fig. 3a). For AgD, the values are 22.2 ns, 5.2 $\mu$s and 4.13 ms (see Fig. 3b). Note that the calculated values are for $J' = 0$ levels. Spontaneous emission from the $J' = 0$ levels is only via the $P(1)$ transition, whereas both $R(0)$ and $P(2)$ transitions are allowed for the $J' = 1$ level. It can be proven that the rotational factor $(S(J', J'')/2J' + 1$ in Eq. 1) for the $P(1)$ transition is equal to the sum of those for the $P(2)$ and $R(1)$ transitions. The difference between spontaneous emission rates from the $J' = 0$ and $J' = 1$ levels of a certain vibrational state is therefore soly determined by the transition frequencies ($\nu_{i,j}$) and is hence negligible.

The vibrational relaxation lifetimes of $X^1\Sigma^+(v'' \geq 1)$ vibrational states for AgH and AgD exceed 20 ms. In comparison, under typical laser-cooling conditions, the rate of optical cycling is required to be at the level of $10^5$ - $10^8$ s$^{-1}$ [18]. Thus, vibrational relaxation is negligible and not included in simulations (see Section IV).

## IV. SIMULATION OF COOLING DYNAMICS

The rate-equation approach is used to simulate the population dynamics of AgH and AgD in the laser-cooling process [24]. The average number of photons scattered by a molecule can be determined from the simulation. For a given energy level $i$, the rate equation for its population $P_i$ can be written as: [12, 50, 51]

$$\begin{aligned} \frac{dP_i}{dt} = &- \sum_{j=1}^{j=i-1} A_{i \rightarrow j} P_i - \sum_{j=1}^{j=i-1} B_{i \rightarrow j} \rho(\omega_{ij}) P_i \\ &- \sum_{j=i+1}^{j=N} B_{j \leftarrow i} \rho(\omega_{ij}) P_i + \sum_{j=i+1}^{j=N} A_{j \rightarrow i} P_j \\ &+ \sum_{j=i+1}^{j=N} B_{j \rightarrow i} \rho(\omega_{ij}) P_j + \sum_{j=1}^{j=i-1} B_{i \leftarrow j} \rho(\omega_{ij}) P_j \end{aligned} \tag{2}$$

where $N$ is the total number of energy levels included in

are related to the $A$ coefficient by

$$B_{i\to j} = B_{i\leftarrow j} = \frac{\pi^2 c^3}{2\hbar\omega_{ij}^3} A_{i\to j} \qquad (3)$$

where $\hbar$ is the reduced Planck constant, and $c$ is the speed of light.

Doppler cooling relies on numerous momentum kicks from the absorption of red-detuned photons counter-propagating to the particle's direction of motion. Given an angular frequency of the detuning $\delta\omega$, the average energy loss per scattering event is $\delta E = \hbar\delta\omega$. The mean number of scattered photons by a molecule in unit time interval, viz., the rate of the scattering events, that can be *achieved* in Doppler cooling is obtained by numerically solving the rate equation (Eq. 2), and then multiplying the population in the excited state of the cycling transition by its total spontaneous emission rate, i.e., summation in the first term of the rate equation (Eq. 2). The mean number of photon scattering events per molecule *required* for cooling is equal to the mean kinetic energy ($E_k$) of pre-laser-cooling molecules, which is determined by the initial temperature of the ensemble, divided by $\delta E$. Note that both cooling and re-pumping laser photons have to be taken into account because they are equivalent in the cooling process. The final temperature that can be achieved by laser cooling in experiments is a function of interaction time, usually limited by population leakage experimental conditions.

In the present work, we simulate the laser-cooling process of AgH and AgD from 25 K to 2 mK. The initial and final temperatures are selected to be the same as in the experimental work on YO [21], Assuming a Maxwell-Boltzmann distribution, these two temperatures correspond to rms velocities ($v_{rms}$) of 76 and 0.68 m/s, respectively. We further assume that the red-detuning $\delta\omega = \Gamma/2$, where $\Gamma = \sum A_{0v''}/(2\pi)$ is the nature linewidth of the laser-cooling transition. The calculation outlined above shows that approximately 73000 scattering events are required to laser-cool AgH or AgD.

Two laser-cooling schemes are proposed (Section II). Total number of scattered photons by each AgH or AgD molecule and the velocity reduction as functions of the interaction time in laser cooling schemes utilizing the $J' = 1 \leftarrow J'' = 0$ and $J' = 0 \leftarrow J'' = 1$ transitions in the $A^1\Sigma^+$ - $X^1\Sigma^+$ (0 - 0) band are plotted in Fig. 5 and 6, respectively. When the $J' = 1 \leftarrow J'' = 0$ transition is used, it takes 22.7 and 18.6 ms to cool AgH and AgD molecules to 2 mK, respectively. The distances of interaction is estimated to be about 124 and 97 cm for AgH and AgD, respectively. In comparison, when the $J' = 0 \leftarrow J'' = 1$ transition is used, the required laser-cooling time is 14.7 ms (AgH) and 13.1 ms (AgD), while the interaction distances are 78 cm (AgH) and 67 cm (AgD). Therefore, the latter scheme has high cooling efficiency. Note that no re-pumping laser is used to return the population on the $v'' = 2$ level to the cooling cycle. Furthermore, in the simulation discussed above, vibrational and rotational decay processes within the $X^1\Sigma^+$



FIG. 4. (Color online) Calculated Franck-Condon factors for transitions between the lowest 10 vibrational levels of $A^1\Sigma^+$ and $X^1\Sigma^+$ states of AgH (a) and AgD (b) molecules.

the model, which are sorted in ascending order ($E_j > E_i$ if $j > i$ and vice versa). $P_i$ and $P_j$ denote populations of the energy levels. $A$'s and $B$'s are Einstein coefficients. Arrows in their subscripts indicate the directions of transitions, with the left (right) state being the higher (lower)-energy one. Therefore, for the $B$ constants, a left (right) arrow in the subscript indicates absorption (stimulated emission). $\omega_{ij}$ is the transition angular frequency between the $i^{th}$ and $j^{th}$ energy levels and $\rho(\omega_{ij})$ is the energy density of the cooling or re-pumping laser at $\omega_{ij}$. In the present simulation, the saturation energy density is used. While the $A$ coefficients (for spontaneous emission) can be calculated using Eq. 1, the $B$ coefficients

FIG. 5. (Color online) Total number of scattered photons and velocity reduction as functions of the interaction time in the laser cooling scheme utilizing the $J' = 1 \leftarrow J'' = 0$ transition in the $A^1\Sigma^+$ - $X^1\Sigma^+$ (0 - 0) band.
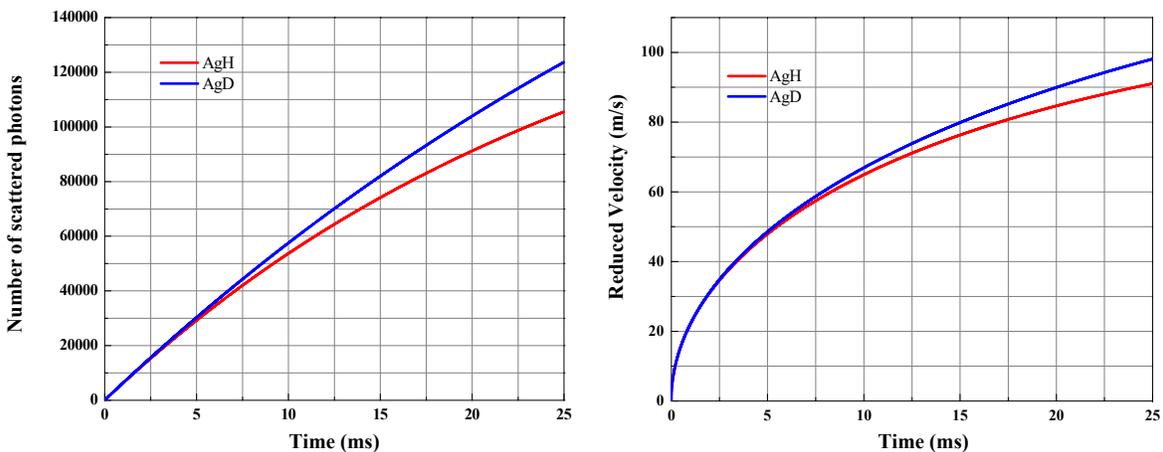


FIG. 6. (Color online) Total number of scattered photons and velocity reduction as functions of the interaction time in the laser cooling scheme utilizing the $J' = 0 \leftarrow J'' = 1$ transition in the $A^1\Sigma^+$ - $X^1\Sigma^+$ (0 - 0) band.

state is ignored in the simulation due to their small rates. Also excluded from the model are blackbody radiation, non-radiative relaxation, predissociation, and photofragmentation processes [24]. The rate of photon scattering decreases gradually as a result of population leakage, mainly to the $v'' = 2$ level. Nevertheless, the population leakage is insignificant because $f_{02}$ is extremely small. The improvement of cooling efficiency by including additional lasers to address this population leakage is minimal.

Nguyen *et al.* introduced a figure of merit (FOM) to evaluate the practicality and efficiency of laser cooling [24]. $FOM = A_{0' \to 0}/(NA_{1 \to 0})$, where $A_{0' \to 0}$ is the Einstein coefficient for the $(v' = 0) \to (v'' = 0)$ electronic relaxation, while $A_{1 \to 0}$ is the Einstein coefficient for the $(v'' = 1) \to (v'' = 0)$ vibrational relaxation. $N$ is the total number of scattered photons for laser-cooling. The FOM for AgH and AgD is 13 and 76, respectively. The difference between the FOMs of AgH and AgD is

mainly due to the smaller vibrational frequency of AgD and hence its smaller $A_{1 \to 0}$. In comparison, the FOM of SrF is 250 [24].

## V. DISCUSSION AND CONCLUSIONS

In the present work, feasibility of utilizing the simplest electronic transition, viz., the $^1\Sigma^+$ - $^1\Sigma^+$ system for direct laser cooling of diatomic molecules is examined using AgH and AgD as examples. *Ab initio* calculations using the internally contracted MRCI method have been carried out to predict the PECs of low-lying electronic states and determine the TDMs for transitions between the ground and the excited electronic states. The calculated molecular constants agree with experimental measurements, where available. The laser cooling process is simulated by numerically solving the rate equations us-

ing the calculated FC factors and radiative lifetimes. The present work confirms that molecules in the $^1\Sigma^+$ - $^1\Sigma^+$ system are favorable candidates for direct laser cooling.

Two laser-cooling schemes are proposed in the present work. The scheme utilizing the $J' = 1 \leftarrow J'' = 0$ transition requires four laser frequencies, while the scheme utilizing the $J' = 0 \leftarrow J'' = 1$ transition requires two. Both schemes are significantly simpler in terms of the number of wavelengths than cooling schemes that involve electronic states with spin multiplicity and/or orbital degeneracy. The simplification is eventually attributed to the simplest energy level structure and transition selection rules of the $A^1\Sigma^+$ - $X^1\Sigma^+$ system.

Comparing the two proposed laser-cooling schemes, the one using the $J' = 0 \leftarrow J'' = 1$ transition is simpler in terms of total number of laser wavelengths and slightly more efficient. However, the other scheme using the $J' = 1 \leftarrow J'' = 0$ transition has the advantage of larger pre-cooling population on the $J'' = 0$ level.

Finally, the prospect of trapping laser-cooled molecules deserves further discussion. Magneto-optical trapping (MOT) is the foundation of present-day ultralow-temperature experiments and the most common method for trapping atoms. Trapping diatomic molecules (SrF)

in a MOT has also been achieved [52, 53]. Trapping AgH or AgD molecules in a MOT would be infeasible due to the vanishingly small $g$ factor for closed-shell molecules in the $^1\Sigma^+$ state. Nevertheless, laser-cooled AgH and AgD molecules can be trapped by a time-varying electric field owing to their large permanent electronic dipole moments. Such technique of trapping polar molecules using the Stark effect has been demonstrated in previous experiments [53, 54].

[1] S. Chu, Rev. Mod. Phys. **70**, 685 (1998).
[2] C. N. Cohen-Tannoudji, Rev. Mod. Phys. **70**, 707 (1998).
[3] W. D. Phillips, Rev. Mod. Phys. **70**, 721 (1998).
[4] H. P. Lüschen, P. Bordia, S. Scherg, F. Alet, E. Altman, U. Schneider, and I. Bloch, Phys. Rev. Lett. **119**, 260401 (2017).
[5] N. Balakrishnan, and A. Dalgarno, Chem. Phys. Lett. **341**, 652 (2001).
[6] A. V. Avdeenkov, D. C. E. Bortolotti, and J. L. Bohn, Phys. Rev. A **69**, 012710 (2004).
[7] V. V. Flambaum, and M. G. Kozlov, Phys. Rev. Lett. **99**, 150801 (2007).
[8] J. P. Yuan, Z. Ji, Z. H. Li, Y. T. Zhao, L. T. Xiao, and S. T. Jia, J. Chem. Phys. **143**, 044311 (2015).
[9] D. DeMille, Phys. Rev. Lett. **88**, 067901 (2002).
[10] T. Köhler, K. Góral, and P. S. Julienne, Rev. Mod. Phys. **78**, 1311 (2006).
[11] K. M. Jones, E. Tiesinga, P. D. Lett, and P. S. Julienne, Rev. Mod. Phys. **78**, 483 (2006).
[12] I. S. Vogelius, L. B. Madsen, and M. Drewsen, Phys. Rev. A **70**, 053412 (2004).
[13] M. D. Di Rosa, Eur. Phys. J. D. **31**, 395 (2004).
[14] T. A. Isaev, S. Hoekstra, and R. Berger, Phys. Rev. A **82**, 052521 (2010).
[15] N. Wells, and I. C. Lane, Phys. Chem. Chem. Phys. **13**, 19018 (2011).
[16] I. C. Lane, Phys. Chem. Chem. Phys. **14**, 15078 (2012).
[17] S. Y. Kang, Y. F. Gao, F. G. Kuang, T. Gao, J. G. Du, and G. Jiang, Phys. Rev. A **91**, 042511 (2015).
[18] Y. F. Gao, and T. Gao, Phys. Chem. Chem. Phys. **17**, 10830 (2015).

[19] E. S. Shuman, J. F. Barry, D. R. Glenn, and D. DeMille, Phys. Rev. Lett. **103**, 223001 (2009).
[20] M. Yeo, M. T. Hummon, A. L. Collopy, B. Yan, B. Hemmerling, E. Chae, J. M. Doyle, and J. Ye, Phys. Rev. Lett. **114**, 223003 (2015).
[21] M. T. Hummon, M. Yeo, B. K. Stuhl, A. L. Collopy, Y. Xia, and J. Ye, Phys. Rev. Lett. **110**, 143001 (2013).
[22] V. Zhelyazkova, A. Cournol, T. E. Wall, A. Matsushima, J. J. Hudson, E. A. Hinds, M. R. Tarbutt, and B. E. Sauer, Phys. Rev. A **89**, 053416 (2014).
[23] B. Hemmerling, E. Chae, A. Ravi, L. Anderegg, G. K. Drayna, N. R. Hutzler, A. L. Collopy, J. Ye, W. Ketterle, and J. M. Doyle, J. Phys. B: At. Mol. Opt. Phys. **49**, 174001 (2016).
[24] J. H. V. Nguyen, C. R. Viteri, E. G. Hohenstein, C. D.Sherrill, K. R. Brown, and B. Odom, New J. Phys. **13**, 063023 (2011).
[25] E. Bengtsson, and E. Svensson, Compt. Rend. **180**, 274 (1925).
[26] P. G. Koontz, Phys. Rev. A **48**, 138 (1935).
[27] L. Gerö, and R. Schmid, Z. Phys. **121**, 459 (1943).
[28] R. C. M. Learner, Proc. R. Soc. London, Ser. A **269**, 327 (1962).
[29] H. Birk, and H. Jones, Chem. Phys. Lett. **161**, 27 (1989).
[30] J. Y. Seto, Z. Morbi, F. Charron, S. K. Lee, P. F. Bernath, and R. J. Le Roy, J. Chem. Phys. **110**, 11756 (1999).
[31] H. A. Witek, T. Nakijima, and K. Hirao, J. Chem. Phys. **113**, 8015 (2000).
[32] H. A. Witek, D. G. Fedorov, K. Hirao, A. Viel, and P.-O. Widmark, J. Chem. Phys. **116**, 8396 (2002).

[33] R. J. Le Roy, D. R. T. Appadoo, K. Anderson, A. Shayesteh, I. E. Gordon, and P. F. Bernath, J. Chem. Phys. **123**, 204304 (2005).

[34] B. K. Stuhl, B. C. Sawyer, D. Wang, and J. Ye, Phys. Rev. Lett. **101**, 243002 (2008).

[35] M. G. Tarallo, G. Z. Iwata, and T. Zelevinsky, Phys. Rev. A **93**, 032509 (2016).

[36] K. P. Huber, and G. Herzberg, Constants of Diatomic Molecules (1979).

[37] E. Hulthèn, and R. V. Zumstein, Phys. Rev. **28**, 13 (1926).

[38] Lan Cheng, private communication (2018).

[39] H. J. Werner, P. J. Knowles, G. Knizia, F. R. Manby, M. Schütz, P. Celani, T. Korona, R. Lindh, A. Mitrushenkov, and G. Rauhut, MOLPRO, a package of ab initio programs, version 2012.1; see http://www.molpro.net.

[40] H. J. Werner, and P. J. Knowles, J. Chem. Phys. **89**, 5803 (1988).

[41] M. Reiher, and A. Wolf, J. Chem. Phys. **121**, 2037 (2004).

[42] M. Reiher, and A. Wolf, J. Chem. Phys. **121**, 10945 (2004).

[43] A. Wolf, M. Reiher, and B. A. Hess, J. Chem. Phys. **117**, 9215 (2002).

[44] R. J. Le Roy, J. Quant. Spectrosc. Radiat. Transfer. **186**, 167 (2017).

[45] E. Bengtsson, and E. Olsson, Z. Phys. **72**, 163 (1931).

[46] T. Okabayashi, and M. Tanimoto, J. Mol. Spectrosc. **204**, 159 (2000).

[47] E. S. Shuman, J. F. Barry, and D. DeMille, Nature (London). **467**, 820 (2010).

[48] Y. You, C. L. Yang, M. S. Wang, X. G. Ma, and W. W. Liu, Phys. Rev. A **92**, 032502 (2015).

[49] W. X. Shi, C. L. Li, H. Y. Meng, J. L. Wei, L. H. Deng, and C. L. Yang, Comput. Theor. Chem. **1079**, 57 (2016).

[50] P. F. Staanum, K. Hojbjerre, P. S. Skyt, A. K. Hansen, and M. Drewsen, Nat. Phys. **6**, 271 (2010).

[51] T. Schneider, B. Roth, H. Duncker, I. Ernsting, and S. Schiller, Nat. Phys. **6**, 275 (2010).

[52] J. F. Barry, D. J. McCarron, E. B. Norrgard, and M. H. Steinecker, Nature **512**, 286 (2014).

[53] F. M. H. Crompvoets, H. L. Bethlem, R. T. Jongma, and G. Meijer, Nature **411**, 174 (2001).

[54] S. Y. T. van de Meerakker, P. H. M. Smeets, N. Vanhaecke, R. T. Jongma, and G. Meijer, Phys. Rev. Lett. **94**, 023004 (2005).